The EMBO Journal vol.3 no.11 pp.2561-2567, 1984

A transposon-like structure related to the δ-endotoxin gene of *Bacillus thuringiensis*

D.Lereclus, J.Ribier[1], A.Klier, G.Menou and M.-M.Lecadet

Laboratoire de Biochimie Microbienne, Institut Pasteur, 28 rue du Docteur Roux, F-75724 Paris Cedex 15, and [1]Laboratoire de Biologie Cellulaire Végétale, Université Paris VII, 2, place Jussieu, F-75251 Paris Cedex 05, France

Communicated by R.Dedonder

A DNA segment (Th-sequence) has been found in several strains of *Bacillus thuringiensis*. This Th-sequence [3 megadaltons (Md)] induces adjacent deletions when it is located in the pAMβ1 plasmid derived from *Streptococcus faecalis*. Electron microscopic examination of reannealed single strands of one plasmid (pMT9) carrying such a deletion revealed that the Th-sequence corresponds to a single-stranded loop (2.8 Md) bounded by a short double-stranded stem (<0.2 Md). Southern blotting experiments established that in *B. thuringiensis* the Th-sequence was generally located on the large plasmid which also harbours the gene coding for the delta-endotoxin (crystal protein). Hybridization and heteroduplex analysis of the extrachromosomal DNA from the *berliner* 1715 strain demonstrated that the crystal gene and the Th-sequence are located in close vicinity on a 42-Md plasmid and that they are separated by a 1.3-Md DNA segment. This DNA segment is repeated in inverted orientation, once immediately adjacent to the Th-sequence and once 1.8 Md beyond the crystal gene. A model for the organization of these DNA sequences inside a transposon-like structure is proposed.

Key words: crystal gene/inverted repeats/location of DNA sequences

Introduction

A common feature of *Bacillus thuringiensis* strains is their capacity to synthesize, during the sporulation phase, the insecticidal δ-endotoxin (crystal protein). This protein represents a major part (~30%) of the total protein synthesized and displays a very specific activity spectrum depending on the strains. Thus, *B. thuringiensis* is a promising organism to develop for biological insect pest control (Dulmage, 1981) and to study the transcription and expression of sporulation genes (Klier *et al.*, 1983; Wong *et al.*, 1983). An important step in this direction has been made by the cloning of the structural gene of the δ-endotoxin from two strains: *kurstaki* HD1 (Schnepf and Whiteley, 1981; Held *et al.*, 1982) and *berliner* 1715 (Klier *et al.*, 1982). In the *berliner* 1715 strain the crystal gene is located both on a large plasmid and on chromosomal DNA. When cloned on the plasmid vector pHV33, only the plasmid gene coded for a toxic polypeptide (Klier *et al.*, 1982). Recently, the diversity and multiplicity of locations of the crystal genes in several strains of *B. thuringiensis* has been reported (Kronstad *et al.*, 1983), but as in the *berliner* 1715 strain it is not yet known whether all of these genes are expressed.

Southern hybridization experiments have previously shown important molecular relationships among the large plasmids [>30 megadaltons (Md)] which generally harbour the crystal gene (Lereclus *et al.*, 1982). From such a plasmid, the 54-Md plasmid of the *kurstaki* KTo strain, we have isolated a 3-Md sequence which is located, with the crystal gene, on several other large plasmids from various *B. thuringiensis* strains (Lereclus *et al.*, 1983). This 3-Md sequence (designated as Th-sequence) was isolated by *in vivo* insertion into the pAMβ1 plasmid of *Streptococcus faecalis* which was used as a conjugative vector.

The *in vivo* cloning of the Th-sequence and the diversity of locations for both this sequence and for the crystal gene prompted us to examine the relationship between these two DNA molecules and to determine whether they could be related to transposable elements. In this paper we report studies, involving mapping with restriction endonucleases and

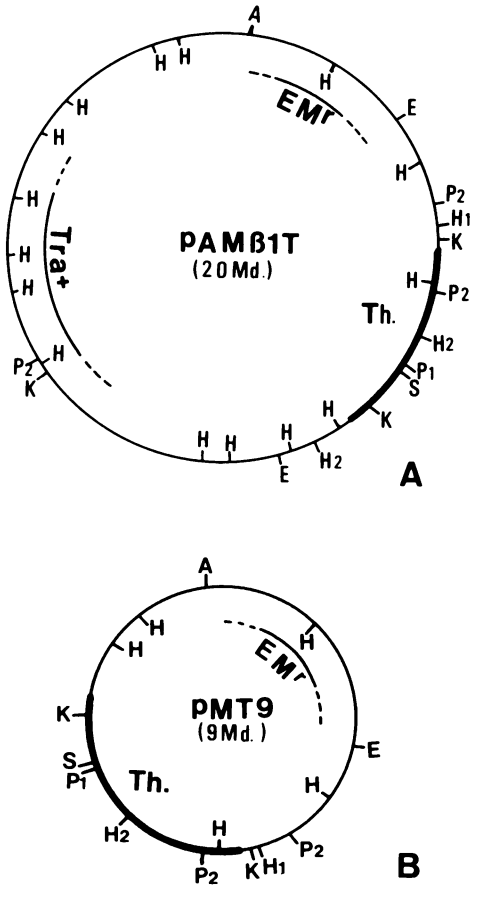

Fig. 1. Localization of the Th-sequence. **(A)** Restriction map of the hybrid plasmid pAMβ1T. **(B)** Restriction map of the deleted plasmid pMT9. Abbreviations used for the restriction endonuclease sites are as follows: A = *Aval*; E = *Eco*RI; H = *Hind*III; H1 = *Hpa*I; H2 = *Hpa*II; K = *Kpn*I; P1 = *Pst*I; P2 = *Pvu*II. The thick line represents the Th-sequence. Em^R and Tra^+ indicate respectively the gene coding for the resistance to erythromycin and the transfer genes located on the pAMβ1 plasmid (thin line) as determined by Le Blanc and Lee (1984).

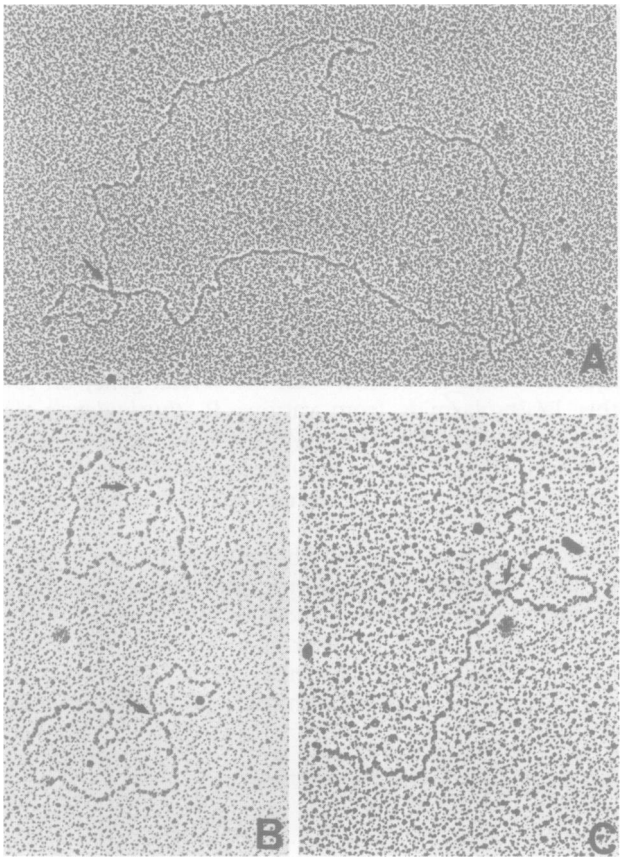

Fig. 2. Electron micrographs of self-annealed single-strands molecules: **(A)** pAMβ1T, **(B)** pMT9 and **(C)** *Eco*RI digest of pMT9. Arrows indicate the junction double-stranded stems.

Southern blotting analysis, done to identify the Th-sequence within the different serotypes of *B. thuringiensis* and to examine its relation with the crystal gene. Moreover electron microscopic analysis allowed a first approach to determine the physical structure of these molecules and their organization on one of the large plasmids of *B. thuringiensis*.

Results

Physical characterization of the Th-sequence

The pAMβ1T plasmid (20 Md) is the result of an *in vivo* insertion of the Th-sequence (3 Md) originating from a 54-Md plasmid of the *B. thuringiensis* KTo strain into the *S. faecalis* pAMβ1 (17 Md) plasmid (Lereclus *et al.*, 1983). The restriction map of pAMβ1T shown in Figure 1A was deduced, after single and double digestions of the DNA with several restriction endonucleases, in comparison with the physical map of pAMβ1 established by Le Blanc and Lee (1984). It appears that insertion of the Th-sequence had occurred within the smaller *Eco*RI fragment of pAMβ1 between the Em^R gene and the transfer genes (Tra^+). More precisely, the Th-sequence is inserted in a set of closely spaced restriction sites (*Hpa*I, *Kpn*I, *Hind*III) within the replication region of pAMβ1 (Le Blanc and Lee, 1984). However, pAMβ1T is not stably maintained in *B. thuringiensis* and derivative non-conjugative plasmids (from 8 to 10 Md), carrying a deletion but specifying resistance to erythromycin and always harbouring the Th-sequence, are generated with a high frequency (Lereclus *et al.*, 1983).

One of these plasmids, the pMT9 plasmid (9 Md), which was isolated by transformation into a *B. subtilis* strain, was analysed further. The restriction map of pMT9 (Figure 1B) shows that it has lost an 11-Md fragment of pAMβ1 including the transfer genes. The deletion is adjacent to one end of the Th-sequence (to the left of the *Kpn*I site of the Th-sequence, Figure 1A). Electron microscopic analysis of reannealed single-strands of pAMβ1T or pMT9, revealed two single-stranded loops joined by a short double-stranded stem (<0.2 Md) (Figure 2A and B), whereas only one single-stranded circle is obtained with the original pAMβ1 plasmid (data not shown). The size of the smaller loop of both pAMβ1T and pMT9 was 2.7 ± 0.4 Md, as estimated from 15 measurements with the single-stranded pAMβ1 molecule (17.4 Md) as a reference (masses indicated correspond to those of double-stranded structures). The reannealed single-strand structure obtained with an *Eco*RI restriction fragment of pMT9 shows a loop of 2.8 ± 0.3 Md, a double-stranded stem (<0.2 Md) and two linear junction fragments (Figure 2C). The respective sizes of the latter fragments (1.8 ± 0.3 Md and 4.5 ± 0.3 Md) are in good agreement with the restriction map of pMT9 (Figure 1B) if we assume that the loop and the stem are produced by self-annealing of the Th-sequence.

Distribution and location of the Th-sequence in B. thuringiensis strains

To study the precise location and the conservation of the Th-sequence among several serotypes of *B. thuringiensis*, we used, as a radioactive probe for Southern blotting analysis, the internal *Kpn*I-*Pvu*II fragment (2 Md) from the Th-sequence of pMT9 (see Figure 1B). This fragment was purified from agarose gels and labelled with ^{32}P. With regard to the location of the Th-sequence within the *kurstaki* KTo strain (serotype 3), Figure 3 shows that the labelled *Kpn*I-*Pvu*II fragment hybridizes, as expected from the restriction map of pMT9 (Figure 1B), with a single *Eco*RI or *Hind*III fragment from the 54-Md plasmid (Figure 3, lanes 1 and 3), but with two *Eco*RI or *Hind*III fragments of total DNA from the KTo strain (Figure 3, lanes 2 and 4). The additional bands found in the digests of the total DNA (containing both plasmid and chromosomal DNA) indicate that the Th-sequence is also present with different junction fragments, in the chromosome of the KTo strain or in a large extrachromosomal DNA molecule not present in the plasmid preparation. These two additional *Eco*RI and *Hind*III fragments have a higher electrophoretic mobility than the plasmid restriction fragments and thus do not originate from a partial digestion of the total DNA. The Th-sequence can therefore originate from either the chromosomal DNA or from the 54-Md plasmid of the KTo strain.

Figure 3 also tells us something concerning the conservation of the Th-sequence among the different serotypes of *B. thuringiensis*. The labelled *Kpn*I-*Pvu*II fragment of the Th-sequence hybridizes with the 35-Md plasmid of the *sotto* strain (serotype 4) (lane 14) and with both the 10-Md and 45-Md plasmids from the *aizawai* strain (serotype 7) (lane 17). We also observed hybridization between the probe and two plasmids of the *berliner* 1715 strain (serotype 1), the pBT42 (42 Md) and the pBT10 (9.5 Md) plasmids (Lereclus *et al.*, 1983). Furthermore, Figure 3 shows that the Th-sequence is present in these plasmids without modification of its restriction map. This can be deduced from the following observations: the *Kpn*I-*Pvu*II fragment which hybridizes with the radioactive probe has the same size in the four strains: *berliner* 1715 (lane 5), KTo (lane 7), *sotto* (lane 15) and

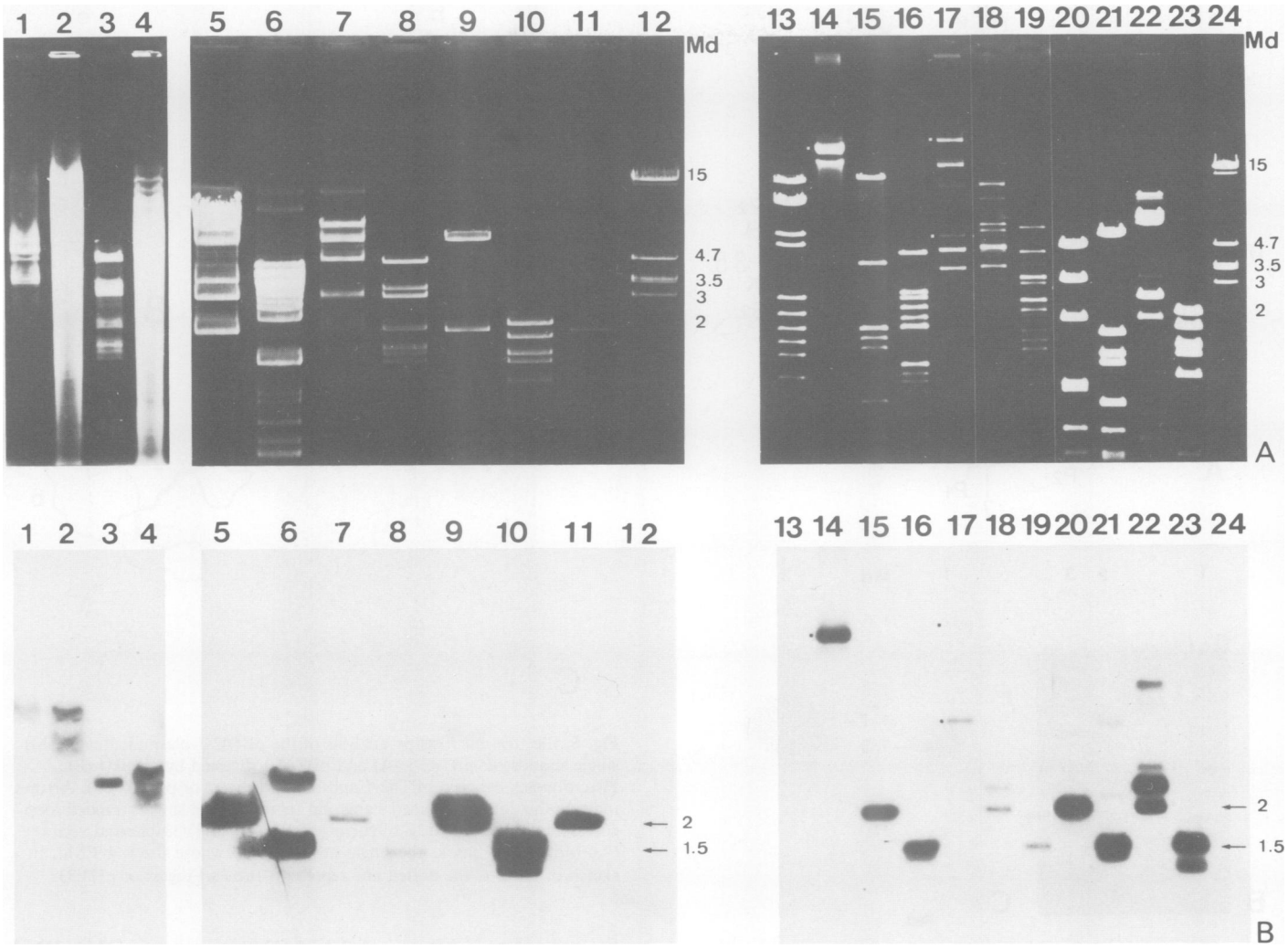

Fig. 3. Location and conservation of the Th-sequence in *B. thuringiensis* strains. **(A)** Electrophoretic pattern of total or plasmid DNA from *B. thuringiensis* strains. **(B)** Autoradiograms of the corresponding blots after hybridization with the ^{32}P-labelled *Kpn*I-*Pvu*II fragment of the Th-sequence **(lane 11)**. *Eco*RI digests of: KTo plasmids **(lane 1)**, KTo total DNA **(lane 2)**. *Hind*III digests of: KTo plasmids **(lane 3)** , KTo total DNA **(lane 4)**. *Kpn*I-*Pvu*II digests of: *berliner* 1715 plasmids **(lane 5)**, KTo plasmids **(lane 7)**, pMT9 (total digest, **lane 9** and partial digest, **lane 22)**, *dendrolimus* plasmids **(lane 13)**, *sotto* plasmid **(lane 15)**, *aizawai* plasmids **(lane 18)**, pBT42-1 **(lane 20)**. *Pst*I-*Hind*III digests of: *berliner* 1715 plasmids **(lane 6)**, KTo plasmids **(lane 8)**, pMT9 **(lanes 10** and **23)**, *sotto* plasmid **(lane 16)**, *aizawai* plasmids **(lane 19)**, pBT 42-1 **(lane 21). Lane 14** represents the 35-Md plasmid of the *sotto* strain (lower band corresponds to the chromosomal DNA). **Lane 17** represents the plasmids of the *aizawai* strain. The respective plasmids of these two strains are indicated by squares on both the agarose gel and the corresponding autoradiogram. The mol. wt. of linear DNA (columns marked Md) was deduced from the *Eco*RI digest of lambda DNA: **lanes 12** and **24**.

aizawai (lane 18). In addition, this size corresponds exactly to the mass of the internal *Kpn*I-*Pvu*II fragment (2 Md) of the Th-sequence (Figure 3, lanes 9, 11 and 22). As deduced from the restriction map of pMT9 (Figure 1B) a *Pst*I-*Hind*III fragment is entirely included in the Th-sequence. When it is hybridized with the radioactive probe this 1.5-Md DNA fragment of pMT9 gives rise to the strongest spots seen in lanes 10 and 23 of Figure 3; the weaker signals correspond to the hybridization between the radioactive probe and the *Pst*I-*Hind*III fragment which is not completely included in the Th-sequence. Figure 3 shows that the internal *Pst*I-*Hind*III fragment which hybridizes with the probe is also present with the same size (1.5 Md) in the four strains: *berliner* 1715 (lane 6), KTo (lane 8), *sotto* (lane 16) and *aizawai* (lane 19); the weaker signals, with variable sizes, correspond to the hybridization between the radioactive probe and the *Pst*I-*Hind*III fragments which are only partially included in the Th-sequence.

The higher mol. wt. fragments which give a positive signal in lanes 18 and 22 (Figure 3B) result from partial digestions of the plasmid preparations (this interpretation is supported by other hybridization experiments which are not presented here). Moreover, these other experiments have verified that the weaker intensity of the spots obtained in lanes 7, 8, 17, 18 and 19 (Figure 3B) is due to the quantity of DNA put on the agarose gel used for transfer and hybridization.

The plasmids of the *berliner* 1715, *kurstaki, sotto* and *aizawai* strains, which hybridize with the Th-sequence, are also those which harbour the crystal gene (Klier *et al.*, 1982; Whiteley *et al.*, 1982; Lecadet and Lereclus, 1984). In contrast, the *dendrolimus* strain, which has the crystal gene located on its chromosomal DNA (Klier *et al.*, 1982), shows no homology at all between the Th-sequence and the *Kpn*I-*Pvu*II digest of its two plasmids (33 and 37 Md) (Figure 3, lane 13).

Th-sequence and crystal gene structural organization in the berliner 1715 strain

To study more thoroughly the relationship between the Th-

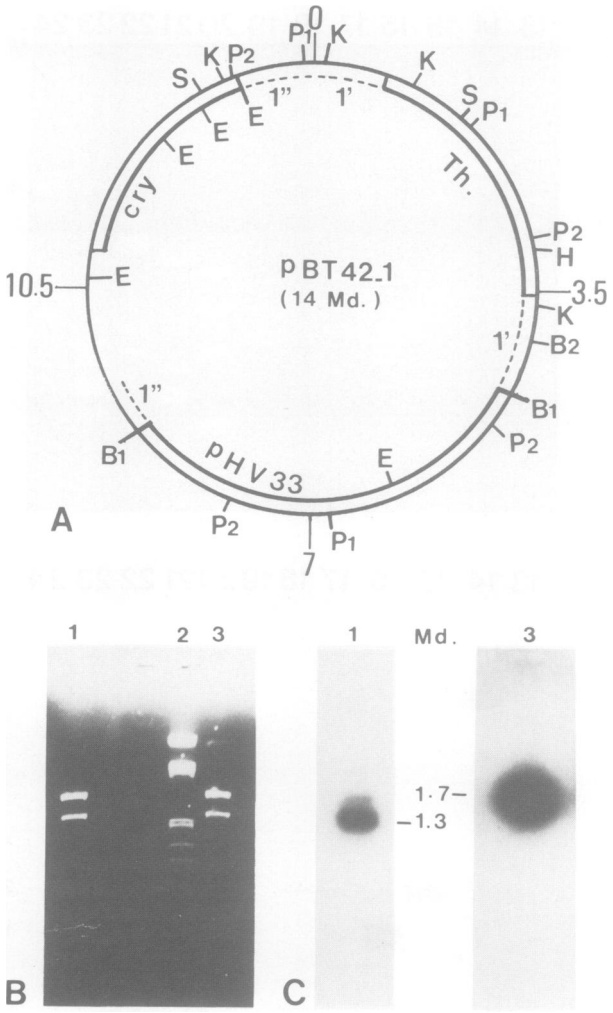

Fig. 4. Localization and organization of the crystal gene and of the Th-sequence on the hybrid plasmid pBT42-1. **(A)** Restriction map. Abbreviations are the same as in Figure 1; additional abbreviations: B1 = *Bam*HI, B2 = *Bgl*II and cry = crystal gene. 0, 3.5, 7 and 10.5 indicate the distances in megadaltons on the restriction map. **(B)** Photograph of ethidium bromide-stained gel containing: **lanes 1** and **3**: *Pst*I digest of the purified *Sst*I fragment mapping at position around 0 on the pBT42-1 restriction map **(panel A)**. **Lane 2**: *Eco*RI-*Hind*III digest of lambda DNA used as mol. wt. marker. **(C)** Autoradiogram of the filter corresponding to **(B)** hybridized with the ^{32}P-labelled *Bam*HI-*Eco*RI fragment mapping at position 10 of the map **(lane 1)** and with the ^{32}P-labelled *Pvu*II fragment mapping at position 3.5 **(lane 3)**. Column Md indicates the mol. wt. of the two DNA fragments which hybridize with the radioactive probes.

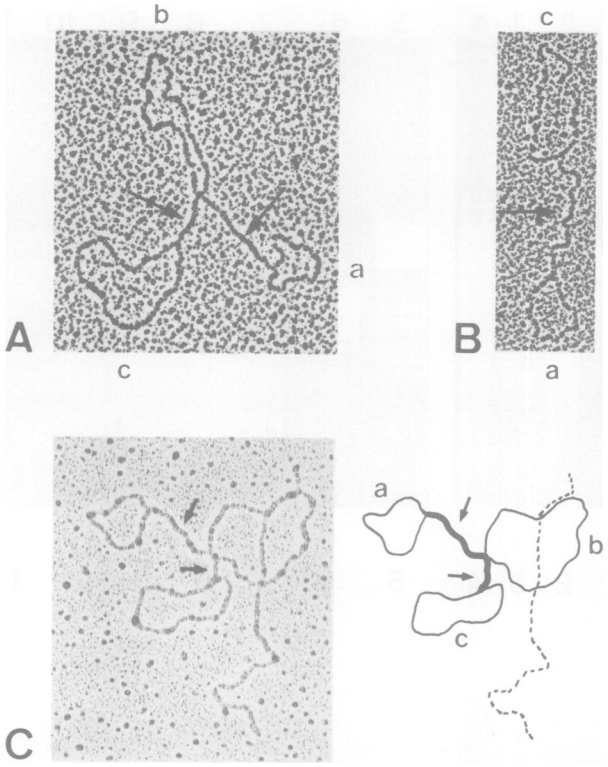

Fig. 5. Electron microscopy analysis of the pBT42-1 plasmid. Reannealed single strands of: pBT42-1 **(A)** and pBT42-1 digested by *Bam*HI **(B)**. Heteroduplex between pBT42-1 and the *Pst*I digest of pHV33 **(C)**. Arrows indicate the double-stranded stems. 'a' represents the single-stranded loop corresponding to 2.8 Md. 'b' corresponds to the pHV33 plasmid vector (4.6 Md) and 'c' marks the single-stranded loop whose size is 4.3 Md. In sketch of **panel C** the dotted line represents the *Pst*I digest of pHV33.

sequence and the crystal gene we have used the hybrid plasmid pBT42-1 (Klier *et al.*, 1982). Containing the structural crystal gene, this plasmid was obtained by ligation of a 9.5-Md *Bam*HI fragment of the 42-Md plasmid (pBT42) from the *berliner* 1715 strain into the *Bam*HI site of the bifunctional vector pHV33 (4.6 Md). In Figure 3 (lanes 20, 21), it can be seen that pBT42-1 contains also the *Kpn*I-*Pvu*II and the *Pst*I-*Hind*III fragment of the Th-sequence. Thus, the Th-sequence originating from the pBT42 plasmid of the *berliner* 1715 strain has been cloned in pBT42-1 together with the crystal gene. By using the previous map of pBT42-1 (Klier *et al.*, 1982), additional Southern blotting and restriction endonucleases analysis allowed us to locate the Th-sequence in pBT42-1 and to establish the physical map presented in Figure 4A. This restriction map shows clearly that the Th-sequence is wholly retained in pBT42-1 and is separated from the crystal gene by an ~1.3-Md DNA sequence. DNA-DNA hybridization experiments (Figures 4B and 4C) have revealed homologies between this 1.3-Md DNA segment and the external junction fragments of the crystal gene and of the Th-sequence. The ^{32}P-labelled *Bam*HI-*Eco*RI fragment, mapping at position 10 Md in Figure 4A, hybridizes with the 1.3-Md *Sst*I-*Pst*I fragment mapping at a position around 13 Md and which contains the segment 1″ (Figures 4B and 4C, lane 1). The ^{32}P-labelled *Pvu*II fragment mapping at position 3.5 Md in Figure 4A, hybridizes with the 1.7-Md *Sst*I-*Pst*I fragment mapping from 0 to 2 Md and containing the segment 1′ (Figures 4B and 4C, lane 3). The significance of the segments marked 1′ and 1″ on Figure 4A will be reported in more detail below.

Electron microscopic analysis of reannealed single strands of pBT42-1 showed three single-stranded loops joined together by two double-stranded stems (Figure 5A). From eight measurements performed on these structures we have deduced the mol. wt. values in terms of double-stranded molecules. The central loop (marked 'b', Figure 5A) flanked by the two stems has a size corresponding to 4.4 ± 0.4 Md. The right stem (0.9 ± 0.1 Md) is joined to a loop marked 'a' of 2.8 ± 0.4 Md and the left stem (0.4 ± 0.1 Md) is linked to a loop marked 'c' of 4.3 ± 0.3 Md. When pBT42-1 digested by *Bam*HI is used for reannealed single-strand formation, two *Bam*HI DNA fragments are observed, one of which is a linear single-stranded *Bam*HI fragment corresponding in size to the pHV33 plasmid (data not shown). The other structure is composed of a long double-stranded segment (1.3 Md)

delimited at each extremity by two single-stranded loops (2.8 Md and 4.3 Md), respectively marked 'a' and 'c' in Figure 5B. This structure corresponds to the 9.5-Md *Bam*HI fragment originating from the pBT42 plasmid of the *berliner* 1715 strain and cloned in pHV33. Thus, it is clear that in the undigested pBT42-1 (Figure 5A), the central loop (marked 'b') corresponds to the pHV33 plasmid flanked by the two double-stranded stems (0.9 and 0.4 Md) originating at its *Bam*HI sites. After cleavage with *Bam*HI the sum of the two double-stranded stems yields the single double-stranded stem of 1.3 Md seen in Figure 5B. This inference is verified by the heteroduplex presented in Figure 5C, which is one of several heteroduplex formations observed between pBT42-1 and the *Pst*I digest of pHV33. This Figure shows an initial region of association between the linear pHV33 molecule and the loop 'b' of pBT42-1.

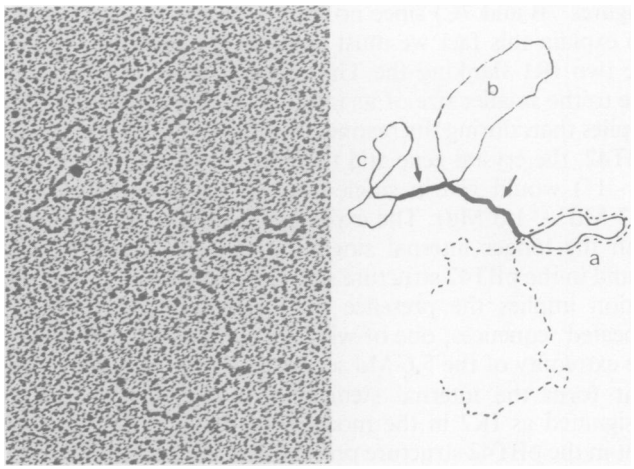

Fig. 6. Heteroduplex between pBT42-1 and the *Eco*RI digest of pMT9. 'a', 'b' and 'c' are defined in the legend of Figure 5. On the tracing, arrows indicate double-stranded stems and the dotted line represents the *Eco*RI digest of pMT9. The single-stranded linear segments correspond to the *Eco*RI junction fragments of pMT9. The double-stranded loop marked 'a' results from the association of the two DNA segments corresponding to the Th-sequences of pBT42-1 and pMT9.

To determine precisely the relative location of the Th-sequence and of the crystal gene in pBT42-1, heteroduplexes were formed between this plasmid and the *Eco*RI digest of pMT9. An electron micrograph of the resulting heteroduplex molecules (Figure 6) shows that the loop marked 'a' (2.8 Md) forms a perfect double-stranded molecule. This proves that in the self-annealed single-strands of pBT42-1 the Th-sequence is located within the 2.8-Md loop. Concerning the precise location of the crystal gene, the molecular hybridization experiments clearly indicated that a 1.3-Md DNA segment was present between the Th-sequence and the crystal gene (see map Figure 4A). Thus we can assume that, in pBT42-1, the crystal gene is contained in the DNA sequence forming the loop of 4.3 Md (marked 'c', Figures 5 and 6).

Finally we looked for the localization of the Th-sequence in the pBT10 and pBT42 resident plasmids of the *berliner* 1715 strain. Since pBT10 and pBT42 harbour the Th-sequence, we expected to find a loop of 2.8 Md in the reannealed single-strands of these two plasmids. Indeed the pBT10 single-stranded molecule (Figure 7A) contains a loop of 2.6 ± 0.4 Md joined by a stem smaller than 0.2 Md to a loop of 6.9 ± 0.5 Md (nine measurements). For this study pBT10 was purified from an agarose gel. In the case of the pBT42 plasmid, from which was derived the hybrid plasmid pBT42-1, reannealed single-strand structures were examined from the total plasmids of the *berliner* 1715 strain using pBT10 as a mol. wt. reference. Among all the species of plasmids, only two kinds of structures (Figures 7B and 7C) were found which corresponded to the previously determined mol. wt. of pBT42 (42 Md) (Lereclus *et al.*, 1982). The sizes of these two

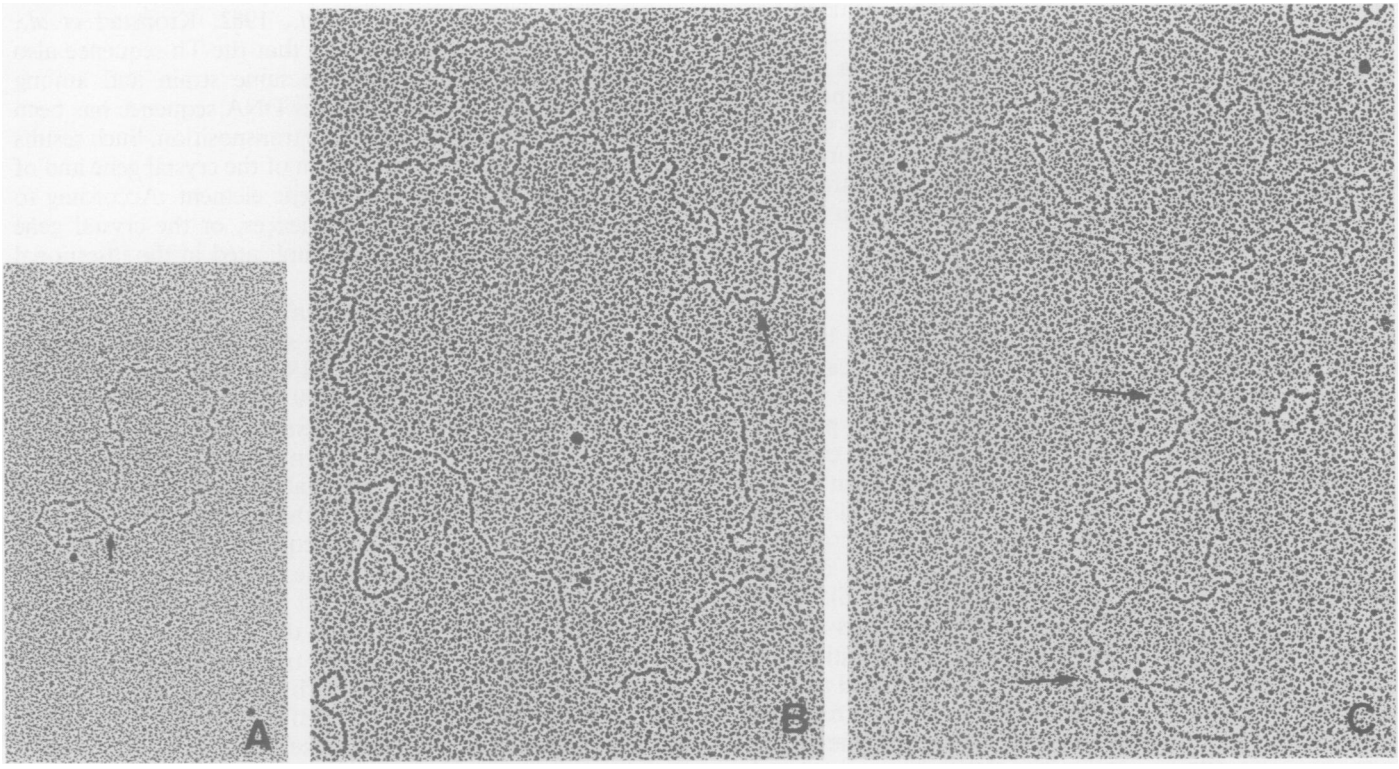

Fig. 7. Electron micrographs of self-annealed single strand molecules. **(A)** pBT10, **(B** and **C)** pBT42. Arrows indicate the double-stranded stems.

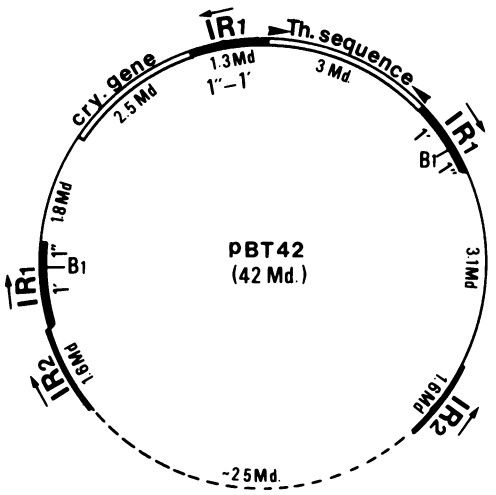

Fig. 8. Model for the structural organization of the IR, crystal gene and Th-sequence in the pBT42 plasmid. The size of each sequence is indicated in megadaltons (Md). The dotted line represents the unexamined part of pBT42 (25 Md). The small arrowheads localized at each extremity of the Th-sequence represent the inverted repeats forming the short double-stranded stem (<0.2 Md) on the self-annealed single strands of the pAMβ1T, pMT9 and pBT10 plasmids. We can note that the true size of the IR1 sequence (independently of the 0.2-Md inverted repeats) corresponds probably to 1.1 Md (1.3−0.2 Md). The arrows indicate the orientation of the IR sequences. B1 indicates the *Bam*HI sites dividing IR1 in two fragments 1′ (0.9 Md) and 1″ (0.4 Md) and which delimit the 9.5-Md DNA fragment cloned in pBT42-1. Other abbreviations are defined in the text.

reannealed single-strand species agree with a double-stranded molecule of 43.5 ± 2.5 Md (eight measurements). In Figures 7B and 7C, the smaller loops of the two self-annealed molecules correspond to a mass of 3.0 ± 0.4 Md with a junction stem of 1.3 ± 0.1 Md. In the molecules whose structure is presented Figure 7C a second double-stranded stem can be seen with a mass of 1.6 ± 0.1 Md. The loop included between the two stems contains two unequal single-stranded fragments (3.1 ± 0.3 Md and 5.8 ± 0.5 Md). We suggest that the smaller distal loop of these molecules corresponds to the self-annealed Th-sequence present in pBT42. In support of this it is important to note that quite similar structures have been obtained with the 35-Md plasmid of the *sotto* strain and with the isolated 45-Md plasmid of the *aizawa* strain (results not shown).

Discussion

The restriction map of pBT42-1 and Southern blotting analysis indicate that a 1.3-Md DNA segment is located between the crystal gene and the Th-sequence. The left part of this DNA-segment (marked 1″ on Figure 4A) presents homology with a DNA segment located on the other extremity of the crystal gene. The right part (marked 1′ on Figure 4A) hybridizes with the external junction fragment of the Th-sequence. These results confirm the electron microscopic examinations which reveal the presence of two double-stranded stems of 0.4 and 0.9 Md (Figures 5 and 6). These stems correspond to the self-annealed 1′ fragments and 1″ fragments. The 1.3-Md DNA segment which is constituted by the sum of the two fragments 1′ and 1″ is designated as IR1. We suggest that in pBT42 the entire IR1 sequence is repeated in inverted orientation on both sides of the crystal gene and of the Th-sequence. IR1 contains a *Bam*HI site between 1′ and 1″ when its orientation is 1′ - 1″. Thus, the two IR1 sequences are not exactly the same in the two orientations. Therefore the *Bam*HI restriction fragment cloned in pBT42-1 contains the following sequence: 1″-crystal gene-1″-1′-Th-sequence-1′.

These results, in addition to those obtained with the pBT42 plasmid (Figures 7B and 7C), lead us to suggest a model (Figure 8) for the structural organization of the IR, crystal gene and Th-sequence in the native pBT42 plasmid. As can be deduced from the reannealed single-strand structure of pBT42-1, the crystal gene, whose size corresponds to 2.5 Md (Klier *et al.*, 1982), is located inside the 4.3-Md sequence itself flanked by two IR1 and which formed the loop 'c' in Figure 6. The pairing of these two IR1 is not observed with pBT42 (Figures 7B and 7C) since no loop of 4.3 Md could be seen. To explain this fact we must assume that the association of the two IR1 flanking the Th-sequence occurs preferentially due to the smaller size of its internal sequence (2.8 Md). This implies that, during the reannealed single-strand formation of pBT42, the crystal gene and the adjacent IR1 (in orientation 1′ - 1″) would give a single-stranded fragment of 5.6 Md (4.3 Md + 1.3 Md). The expected size is in close agreement with the longer internal single-stranded sequence (5.8 Md) found in the pBT42 structure shown in Figure 7C. This observation implies the presence of a second pair of inverted repeated sequences, one of which is contiguous to the IR1 at the extremity of the 5.6-Md sequence. These inverted repeats that form the internal stem of 1.6 Md (Figure 7C) are designated as IR2 in the model (Figure 8). We can assume that in the pBT42 structure presented in Figure 7B the pairing of the two IR2 has not occurred. This model involves the presence of three copies of IR1 which explain the cloverleaf structure of the self-annealed pBT42-1 (Figures 5A and 5C) and the 1.3-Md double-stranded stem obtained with pBT42 (Figures 7B and 7C).

Concerning the transposition properties of these DNA sequences, some observations should be mentioned. First, the crystal protein gene is present on more than one plasmid within several strains (Klier *et al.*, 1982; Kronstad *et al.*, 1983). Secondly, we showed here that the Th-sequence also has multiple locations inside the same strain and among several serotypes. Furthermore this DNA sequence has been isolated consecutively to an *in vivo* transposition. Such results can be explained by the localization of the crystal gene and of the Th-sequence on a mobile genetic element. According to this hypothesis either the IR sequences, or the crystal gene and the Th-sequence, might be implicated in the insertional functions.

Although our experimental data do not bear directly on this last point, we note that the Th-sequence is found after *in vivo* insertion without the IR1 or IR2 sequences. Indeed, the Th-sequence inserted in the pMT9 plasmid presents only a short IR (<0.2 Md) at each extremity, as is the case in the native pBT10 plasmid. This is reminiscent of the Tn3-like transposons for which the terminal IR sequences are 40 bp long (Heffron, 1983). Moreover, these transposons have approximatively the size of the Th-sequence (3 Md) and one of them, Tn551, has been found in the Gram-positive organism, *Staphylococcus aureus* (Khan and Novick, 1980). Another characteristic of the Tn3 family is the formation of adjacent deletions at the extremity of the transposon. We observed that the Th-sequence produced such deletions with a high frequency when it is located in pAMβ1T. Although these observations suggest that the Th-sequence possesses a transposition activity we have no direct evidence of this, nor do we have an indication of the function of this genetic element. However,

we have clearly shown that the Th-sequence is located on several plasmids of *B. thuringiensis* strains that harbour the crystal gene and that this sequence is conserved without apparent modification among serotypes which differ in the specificity of the δ-endotoxin. This is in strong contrast to the *dendrolimus* strain for which a chromosomal location of the crystal gene has been suggested (Klier *et al.*, 1982). In this strain the Th-sequence is not found on the large plasmids.

Thus, the results presented here indicate a close relationship between the Th-sequence and the crystal protein gene. These, together with the IR1 and IR2 sequences, constitute a set of DNA sequences with striking similarities to the organization of the heat-labile and heat-stable enterotoxin genes in an unique plasmid of several clinical strains of *E. coli* (Yamamoto and Yokota, 1981). In this complex arrangement of genes the Th-sequence might play an important role since it is conserved among *B. thuringiensis* species.

Materials and methods

Bacterial strains and growth conditions

The *berliner* 1715, *kurstaki* KTo, *dendrolimus* and *aizawai* strains of *B. thuringiensis* originated from the Centre O.I.L.B. (Institut Pasteur). The *sotto* strain was kindly provided by R.M.Faust. *B. subtilis* QB625 (*sacB209, trpC2, hisA1*) was constructed in the laboratory. For DNA preparations *B. thuringiensis* and *B. subtilis* strains were grown in Luria broth at 30 and 37°C respectively.

Transformation procedure

B. subtilis was transformed as described by Niaudet and Ehrlich (1979). Transformed cells were selected on Luria-agar plates containing 25 μg erythromycin/ml.

Preparation and analyses of DNA

Chromosomal DNA was purified as previously reported (Klier *et al.*, 1973).

Plasmid DNA was extracted from large culture volumes (1 – 2 litres) according to the alkaline denaturation procedure (Birnboim and Doly, 1979) with the modifications reported previously (Lereclus *et al.*, 1982). Plasmids were purified by caesium chloride gradient equilibrium centrifugation in the presence of ethidium bromide.

DNA preparations were analysed by horizontal 0.6 or 0.7% agarose gel electrophoresis. Electrophoretic migration was carried out at 5 V/cm for 5 h in Tris 40 mM, sodium acetate (3 H_2O) 20 mM, EDTA 2 mM, adjusted to pH 7.8 with acetic acid. DNA molecules were visualised by u.v. irradiation after ethidium bromide staining.

Recovery of plasmids or of DNA fragments from agarose gel was obtained by electro-elution in a dialysis bag. The purification of the DNA molecules recovered was carried out with Elutip-d columns (Schleicher and Schüll).

^{32}P-labelling and hybridization procedures

DNA molecules were labelled by nick-translation according to Rigby *et al.* (1977) in the presence of 20 μCi [α-^{32}P]dCTP and of [α-^{32}P]dATP (New England Nuclear, Boston, MA; 400 Ci/mM). Generally the resulting labelled DNA presented a specific radioactivity ranging from 1 to 3 x 10^7 c.p.m./μg.

Hybridization experiments were carried out after electrophoresis of DNA, using the Southern technique, as previously described (Lereclus *et al.*, 1982).

Electron microscopy

The method used in the formation of self-annealed or heteroduplex molecules is that described by Davis *et al.* (1971). Methods for analysis and measurements of the DNA molecules have been previously reported (Lereclus *et al.*, 1982). The micrographs correspond to a 32 000 x magnification of the DNA molecules.

Acknowledgements

We are grateful to Dr. R.Rippka-Herdmann and Dr. P.Bray for revising the English manuscript and to Dr. R.Dedonder and Dr. S.Puiseux-Dao in whose laboratories this work was conducted. We wish to thank Dr. J.Moreau for the measurements with the Packard digitiser. This work was supported by research grants from the Centre National de la Recherche Scientifique (ATP Microbiologie), from the Commissariat à l'Energie Atomique and from the Fondation pour la Recherche Médicale.

References

Birnboim,H.C. and Doly,J. (1979) *Nucleic Acids Res.*, **7**, 1513-1523.
Davis,R.W., Simon,M. and Davidson,N. (1971) *Methods Enzymol.*, **21**, 413-428.
Dulmage,H.T. (1981) in Burges,H.D. (ed.), *Microbial Control of Pests and Plant Diseases, 1970–1980*, Academic Press, pp. 193-222.
Heffron,F. (1983) in Shapiro,J. (ed.), *Mobile Genetic Elements*, Academic Press, NY, pp. 223-260.
Held,G.A., Bulla,L.A.,Jr., Ferrari,E., Hoch,J., Aronson,A.I. and Minnich, S.A. (1982) *Proc. Natl. Acad. Sci. USA*, **79**, 6065-6069.
Khan,S.A. and Novick,R.P. (1980) *Plasmid*, **4**, 148-154.
Klier,A., Lecadet,M.-M. and Dedonder,R. (1973) *Eur. J. Biochem.*, **36**, 317-327.
Klier,A., Fargette,F., Ribier,J. and Rapoport,G. (1982) *EMBO J.*, **1**, 791-799.
Klier,A., Parsot,C., Rapoport,G. (1983) *Nucleic Acids Res.*, **11**, 3973-3987.
Kronstad,J.W., Schnepf,H.E. and Whiteley,H.R. (1983) *J. Bacteriol.*, **154**, 419-428.
Le Blanc,D.J. and Lee,N.L. (1984) *J. Bacteriol.*, **157**, 445-453.
Lecadet,M.-M. and Lereclus,D. (1984) in Alouf,J.E., Freer,J.H., Fehrenbach,F.J. and Jeljaszewicz,J. (eds.), *Bacterial Protein Toxins, FEMS Symposium 1983*, Academic Press, London, pp. 147-154.
Lereclus,D., Lecadet,M.-M., Ribier,J. and Dedonder,R. (1982) *Mol. Gen. Genet.*, **186**, 391-398.
Lereclus,D., Menou,G. and Lecadet,M.-M. (1983) *Mol. Gen. Genet.*, **191**, 307-313.
Niaudet,B. and Ehrlich,S.D. (1979) *Plasmid*, **2**, 48-58.
Rigby,P.W.J., Dieckmann,M., Rhodes,C. and Berg,P. (1977) *J. Mol. Biol.*, **113**, 237-251.
Schnepf,H.E. and Whiteley,H.R. (1981) *Proc. Natl. Acad. Sci. USA*, **78**, 2893-2897.
Whiteley,H.R., Kronstad,J.W. and Schnepf,H.E. (1982) in *Basic Biology of Microbial Larvicides of Vectors of Human Diseases*, WHO, UBC, Genève, pp. 147-156.
Wong,H.C., Schnepf,H.E. and Whiteley,H.R. (1983) *J. Biol. Chem.*, **258**, 1960-1967.
Yamamoto,T. and Yokota,T. (1981) *J. Bacteriol.*, **145**, 850-860.

Received on 6 April 1984; revised on 30 July 1984